THE UNIVERSITY OF MICHIGAN
COLLEGE OF ENGINEERING
Department of Electrical Engineering
Space Physics Research Laboratory

Scientific Report No. MS-3

THE THERMOSPHERE PROBE EXPERIMENT

D. R. Taeusch
G. R. Carignan
H. B. Niemann

ORA Project 04304

under contract with:

NATIONAL AERONAUTICS AND SPACE ADMINISTRATION
GODDARD SPACE FLIGHT CENTER
CONTRACT NO. NASr-15
GREENBELT, MARYLAND

administered through:

OFFICE OF RESEARCH ADMINISTRATION ANN ARBOR

February 1964

TABLE OF CONTENTS

LIST OF FIGURES

1. DESCRIPTION OF EXPERIMENT

1.1 INTRODUCTION

The thermosphere probe (TP) experiment described herein is the result of a research effort implemented by this laboratory under contract with the NASA Goddard Space Flight Center, Aeronomy and Meteorology Division. The purpose of this effort was to provide an ejectable rocket-borne system capable of making simultaneous direct measurements of gas temperature and density, ion and electron density, and electron temperature in the earth's atmosphere in the altitude region between 100 and 350 km, a region within the thermosphere. The primary mission of the experiment is to fill the present measurement gap in this general altitude region which is above the altitude capability of the grenade, falling sphere and pitot-static techniques, and below the altitude of usual satellite measurements.

The TP incorporates a pressure gauge, which can be either a partial pressure sensor, a total pressure sensor, or both; and a cylindrical and a hemispherical electrostatic probe.[1] This complement of instruments provides data for the determination of the previously mentioned desired atmospheric parameters.

The ejectable system was chosen for the purpose of removing the TP from the environment of the launch vehicle, similar to the established "Dumbbell" technique,[1] and to permit a tumbling motion to be imparted to the package, independent of the launch vehicle.

The following report describes the theoretical background and techniques utilized in obtaining the gas temperature and density data from the flight of NASA 6.06 on November 20, 1962. Only those engineering particulars that bear directly on the actual measurement of the desired quantities required for data analysis are described in this report. A comprehensive engineering report of the system will be written under separate cover.

1.2 THE THERMOSPHERE PROBE

The TP is a cylindrical instrument 6 in. in diam, 26 in. long and weighs 33 lb. A photograph of the assembled instrument is shown in Fig. 1. One end of the cylinder contains the omegatron gauge with its circular orifice on the cylindrical axis; the other end of the cylinder is a 6-in. hemisphere which is one electrode of the electrostatic probe system. The center section contains the sun-earth aspect sensor, a small cylindrical electrostatic probe and the telemetry antennae. The outer structure of the probe is made of stain-

less steel and the assembled instrument is vacuum sealed. The probe system is completely self-contained providing its own power supply, measuring sensors, signal conditioning, and transmission equipment.

1.3 EJECTION AND TUMBLE SYSTEM

The ejection nose cone system is shown in Fig. 2. The clamshell-type nose cone halves, which provide the aerodynamic shape of the rocket during powered flight are hinged to the base of the enclosure and are held together against the force of two springs by a magnesium ring which is pyrotechnically fractured to effect opening. The TP rests on a spring-loaded plunger within the enclosure. The plunger is held depressed against the spring force by a latch mechanically linked to a nose cone half so that opening of the nose cone releases the latch, freeing the plunger, which, operating against the compressed spring, ejects the TP from the opened enclosure. A negator motor (constant force spring), with 8 ft of cable is mounted below the plunger. One end of the cable is fastened to the top side of the TP. As the TP leaves the vehicle, it is tumbled in the plane containing the cable hook and the center of gravity. When the TP has tumbled approximatly 90°, the cable releases and is reeled back into the vehicle.

The ejection system causes the TP to separate from the nose cone at about 4 fps and the negator or constant force spring imparts the tumble motion with a period of 1.8 sec. The roll period is noncontrolled and is the resultant of the roll period of the rocket at ejection. The opening of the nose cone halves prior to ejection provides an effective despin mechanism assuring a roll rate substantially less than the tumble rate. Thus, with a low roll rate and a moment of inertia ratio of more than 50, the TP can be considered to be tumbling in the plane of the cylindrical axis.

2. ASPECT DETERMINATION

2.1 INTRODUCTION

The analysis of the neutral particle-pressure measurement requires that the orientation of the pressure-gauge orifice, with respect to the velocity vector, be known. For this purpose, the TP experiment utilizes a sun-earth aspect sensor.[2]

In effect, the sun aspect sensor views a fan, 160° wide, the plane of which is oriented perpendicular to the long axis of the TP. As the TP tumbles, and rolls, the fan sweeps out a solid angle of 4π steradians, thereby viewing the sun at periodic intervals. The output of the sun sensor yields the roll position of the TP at the time the sun is viewed. A thorough treatment of the mechanics of the sun-earth aspect sensor system can be found in Ref. 2.

As was described in a previous section of this report, the ejection system for the TP is designed to decrease the roll rate and tumble the instrument in the plane containing the cylindrical axis. Since there are no external torques on the TP after ejection, it will be assumed that the angular momentum vector, $\bar{L}$, for the system will remain fixed in inertial space. For the determination of $\bar{L}$, the tumble period and roll period must be known.

2.2 TUMBLE PERIOD

Two independent methods for the determination of the TP tumble period are available. The period between successive sun pulses can be read more accurately and is used for the tumble-period measurement, with the period between pressure maxima providing confirmation of the results. The tumble period is measured with an error of less than 2 msec (~1 part in 500).

2.3 ROLL PERIOD

Each cycle of the tumble motion causes the sun sensor to generate an output which is a function of the TP roll position. The roll rate is determined by the following analysis of this information:

Let

ω = roll rate (deg/sec)

θ = roll position of TP

k = an integer (0,1,2,...)

n = number of 1/2 tumble periods

t = time

then

$$\omega = \frac{\pm\theta_{(n+2)} - \theta_n \pm k\ 360^\circ}{t_{(n+2)} - t_n}$$

where

$t_{(n+2)} - t_n$ is simply the tumble period.

The roll rate, in deg/sec, is equal to the number of degrees the TP has apparently rolled in one tumble period ($\pm\theta_{n+2} - \theta_n$), plus the number of complete cycles it has rolled ($\pm k\ 360^\circ$), divided by the tumble period—the time between roll position data inputs, θ_{n+2} and θ_n. The plus or minus signs are a consequence of the uncertainty in roll direction.

In the TP application, since the tumble period is less than the roll period, k is 0 and the equation becomes $\pm\theta_{n+2} - \theta_n / t_{n+2} - t_n$. Any pair of sensor outputs provide a solution; therefore, successive solutions can be used to prove the assumption k = 0 and also to indicate the correct sign in $\pm\theta_{n+2}$.

2.4 ORIENTATION ANALYSIS

Figure 3 shows the coordinate system used for the determination $\overline{L}$. It is a right cartesian-coordinate system in which the z axis is pointing at the sun.

The $\overline{TP_1}$, and $\overline{TP_2}$ vectors describe the position of the TP cylinder axis, the direction being that of the normal to the orifice of the pressure gauge. $\overline{TP_1}$ is the position of the TP at the time it is closest to the velocity vector, i.e., the time a maximum pressure reading is recorded. $\overline{TP_2}$ is the position of the TP at the time a sun pulse is received. $\overline{TP_2}$ is in the x-y plane since the sun sensor is perpendicular to the axis to the TP.

The angle γ_1 is the angle between $\overline{TP_1}$ and $\overline{TP_2}$. It is determined by measuring the time difference, Δt, between a peak pressure reading and a sun pulse. The angle γ_1 is then given by:

$$\gamma_1 = 360^\circ \times \frac{\Delta t}{\text{tumble period}} .$$

The angle γ_2 is the half angle of the cone, about the z axis, of all possible angular momentum vectors. This is determined by the following analysis:

Let

t = time

n = number of 1/2 tumble periods

ω = roll rate

γ_2 = cone half angle of $\bar{L}$ from z axis

Θ = sun sensor roll position

Then, assuming that the roll rate is less than the tumble rate:

$$2\gamma_2 = \Theta_{n+1} - \Theta_n + \omega(t_{n+1}-t_n) .$$

This equation is not obvious, but simply says that once one knowns Θ_n and where the sun sensor has rolled to in half a tumble period, Θ_{n+1} can only be the received output for one plane of tumble with respect to the sun vector. γ_2 is the half angle of the cone of possible angular momentum vectors about z.

2.5 ORIENTATION EQUATIONS

Referring to Fig. 3 which shows the vectors to be determined, the equations to be solved are the following:

Assuming the TP is tumbling in a plane, we get:

$$\overline{TP}_1 \cdot \bar{L} = \overline{TP}_2 \cdot \bar{L} = 0. \qquad (2.5.1)$$

From our previous definition of γ_1:

$$\overline{TP}_1 \cdot \overline{TP}_2 = \cos \gamma_1 . \qquad (2.5.2)$$

Since the $\overline{TP}_1$ vector is tangent to the cone of minimum angle of attack, we can say:

$$\bar{L} \cdot \overline{TP_1} \times \bar{V} = 0 . \qquad (2.5.3)$$

The minimum angle of attack, α, is then given by:

$$\frac{\overline{TP_1} \cdot \bar{V}}{|\bar{V}|} = \cos \alpha \qquad (2.5.4a)$$

or

$$\frac{\bar{L} \cdot \bar{V}}{|\bar{V}|} = \sin \alpha . \qquad (2.5.4b)$$

Assuming all vectors, except $\bar{V}$, are unit vectors.

Using typical spherical coordinates, Θ measured from the z axis and ϕ, the angle in the x-y plane, measured counterclockwise from the x axis, we can solve the above four equations for the unknown quantity ϕ_L, the ϕ position of $\bar{L}$. Θ_L is by definition equal to γ_2.

The solutions are:

$$\cos(\phi_1-\phi_2) = \left[\frac{A^2+\cos^2\gamma_1}{A^2+1}\right]^{1/2} \qquad (2.5.5)$$

where

$$A = \frac{\cos \gamma_1}{\cos \gamma_2}$$

$$\sin \Theta_1 = \frac{\cos \gamma_1}{\cos(\phi_1-\phi_2)} \qquad (2.5.6)$$

$$\phi_2-\phi_L = \pm \frac{\pi}{2} \qquad (2.5.7)$$

$$\sin(\phi_1-\phi_L) = \frac{BC \pm \sqrt{B^2-C^2+1}}{B^2+1} . \qquad (2.5.8a)$$

For $\phi_2-\phi_L = \frac{\pi}{2}$

$$\sin(\phi_1-\phi_V) = \frac{-BC \pm \sqrt{B^2-C^2+1}}{B^2+1} \qquad (2.5.8b)$$

for $\phi_2-\phi_L = -\frac{\pi}{2}$

where

$$B = \frac{\sin^2(\phi_1-\phi_2)+\cot^2\gamma_2}{\sin(\phi_1-\phi_2)\cos(\phi_1-\phi_2)}$$

$$C = \frac{\cot\gamma_2 \cot\Theta_V}{\sin(\phi_1-\phi_2)} .$$

The above equations yield eight solutions for ϕ_L.

If this analysis is carried out at two or more times during the flight, with data input from the sun sensor, only one of the eight solutions will yield the same ϕ_L each time. This then is the correct ϕ_L, and the angular momentum vector is known.

2.6 DIRECT METHOD OF OBTAINING α

Another method of finding α directly is discussed below. This method gives a more understandable physical picture of the TP's motion and yields α directly for each time sun sensor data are available.

Figure 4 shows the plane of tumble (shaded plane) and its relationship to the measured quantities, γ_1 and γ_2. The cone half angle $\overline{AD}$ is equal to $(\pi/2)-\gamma_2$. It is the cone to which all possible tumble planes must be tangent. $\overline{EB}$ is the angle γ_1, the angle measured between a sun-pulse and a peak-pressure measurement (at B). The circle about the sun vector of radius $\overline{AB}$ describes the locus of all possible positions of the TP when a peak-pressure measurement was received. The criterion for a solution is that the tumble plane must be tangent to the cone $\overline{AD}$ and must be tangent to a cone about the velocity vector (cone half angle $\overline{BC}$) at a point on the cricle of radius AB (Θ_1 of our previous analysis). The angle BC is by definition the minimum angle of attack α, to be solved for.

The problem then is to solve the spherical triangles for the angle BC = α in terms of the known quantities AB = Θ_1, BD = $(\pi/2)-\gamma_1$, AC = Θ_V, AD = $(\pi/2)-\gamma_2$ (see Fig. 5).

$$\cos\overline{AC} = \cos\overline{BC}\cos\overline{AB} + \sin\overline{BC}\sin\overline{AB}\cos(90°+\mu)$$

or

$$\cos\overline{AC} = \cos\overline{BC}\cos\overline{AB} - \sin\overline{BC}\sin\overline{AB}\sin\mu \qquad (2.6.1)$$

also

$$\cos\overline{AB} = \cos\overline{AD}\cos\overline{BD} + \sin\overline{AD}\sin\overline{BD}\cos 90°$$

or

$$\cos \overline{AB} = \cos \overline{AD} \cos \overline{BD} . \qquad (2.6.2)$$

Now, from the sine law:

$$\frac{\sin \overline{AB}}{\sin \frac{\pi}{2}} = \frac{\sin \overline{AD}}{\sin \mu}$$

or

$$\sin \overline{AB} = \frac{\sin \overline{AD}}{\sin \mu} . \qquad (2.6.3)$$

Substituting Eqs. (2.6.2) and (2.6.3) into Eq. (2.6.1), we get:

$$\cos \overline{AC} = \cos \overline{BC} \cos \overline{AD} \cos \overline{BD} - \sin \overline{BC} \sin \overline{AD} . \qquad (2.6.4)$$

Rearranging

$$\cos \overline{AC} - \cos \overline{BC} \cos \overline{AD} \cos \overline{BD} = -\sqrt{1-\cos^2 \overline{BC}} \sin \overline{AD}.$$

Squaring both sides

$$\cos^2 \overline{AC} + \cos^2 \overline{BC} \cos^2 \overline{AD} \cos^2 \overline{BD} - 2 \cos \overline{AC} \cos \overline{BC} \cos \overline{AD} \cos \overline{BD}$$

$$= \sin^2 \overline{AD} - \cos^2 \overline{BC} \sin^2 \overline{AD} .$$

Rearranging

$$\cos^2 \overline{BC}[\cos^2 \overline{AD} \cos^2 \overline{BD} + \sin^2 \overline{AD}] - 2 \cos \overline{BC}(\cos \overline{AC} \cos \overline{AD} \cos \overline{BD})$$

$$+ (\cos^2 \overline{AC} - \sin^2 \overline{AD}) = 0 .$$

Let

$$\ell = \cos^2 \overline{AD} \cos^2 \overline{BD} + \sin^2 \overline{AD} = \cos^2 \left(\frac{\pi}{2} - \gamma_2\right) \cos^2 \left(\frac{\pi}{2} - \gamma_1\right) + \sin^2 \left(\frac{\pi}{2} - \gamma_2\right)$$

$$m = \cos \overline{AC} \cos \overline{AD} \cos \overline{BD} = \cos \theta_V \cos \left(\frac{\pi}{2} - \gamma_2\right) \cos \left(\frac{\pi}{2} - \gamma_1\right)$$

$$n = \cos^2 \overline{AC} - \sin^2 \overline{AD} = \cos^2 \theta_V - \sin^2 \left(\frac{\pi}{2} - \gamma_2\right)$$

$$\ell \cos^2 \overline{BC} - 2m \cos \overline{BC} + n = 0$$

and

$$\cos \overline{BC} = \frac{m \pm \sqrt{m^2 - \ell n}}{\ell} \quad . \tag{2.6.5}$$

This analysis was carried out with the assumption that the position of the TP at minimum angle of attack was describable in the top hemisphere of the sun coordinate system shown in Fig. 4. If the TP is positioned on the bottom hemisphere [$\overline{AB} > (\pi/2)$] then the angle $\overline{BD}$ is [$(\pi/2)+\gamma_1$)].

For $\overline{AB} < \frac{\pi}{2}$, $\gamma_2 < \frac{\pi}{2}$

$$\ell = \sin^2\gamma_2 \sin^2\gamma_1 + \cos^2\gamma_2$$

$$m = \cos \Theta_V \sin \gamma_2 \sin \gamma_1$$

$$n = \cos^2\Theta_V - \cos^2\gamma_2$$

and for $\overline{AB} > \frac{\pi}{2}$, $\gamma_2 < \frac{\pi}{2}$

$$\ell = \sin^2\gamma_2 \sin^2 \gamma_1 + \cos^2\gamma_2$$

$$m = - \cos \Theta_V \sin \gamma_2 \sin \gamma_1$$

$$n = \cos^2\Theta_V - \cos^2\gamma_2$$

where

$$\cos \alpha = \frac{m \pm \sqrt{m^2 - \ell n}}{\ell} \quad . \tag{2.6.6}$$

3. DATA REDUCTION

3.1 DENSITY VS. ALTITUDE--DATA ANALYSIS

The pressure relationship across the orifice of a pressure gauge mounted within a moving, rotating body in a free-molecular-flow region in a planetary atmosphere, is given by the thermal transpiration equation as modified by drift velocity considerations.[3]

From Ref. 3

$$\frac{P_i}{P_o} = \sqrt{T_i/T_o}\ f(s) \qquad (3.1.1)$$

where

$f(s) = e^{-s^2} + \sqrt{\pi}s(1+\mathrm{erf}s)$

$s = V \cos \beta/u$

$u = \sqrt{2kT/m}$

P = pressure

T = temperature

V = vehicle velocity

β = angle between the normal to the pressure-gauge orifice and the velocity vector

u = most probable thermal velocity for molecules of mass m

i = subscript denoting quantities inside the pressure gauge

o = subscript denoting quantities outside the pressure gauge

For the TP experiment, the pressure gauge is tumbling in a plane which is at an angle α (minimum angle) from the velocity vector. Considering the maximum change in pressure during one tumble period:

$$P_{i_{max}} - P_{i_{min}} = P_o \sqrt{T_i/T_o} \; [f(s)-f(-s)] \qquad (3.1.2)$$

since

$$f(+s) - f(-s) = \sqrt{\pi}\, s[\mathrm{erf}(s)-\mathrm{erf}(-s)] = 2\sqrt{\pi}\, s \; .$$

We get:

$$P_{i_{max}} - P_{i_{min}} = 2P_o \sqrt{\pi}\, s \sqrt{T_i/T_o} = \Delta P_i \; . \qquad (3.1.3)$$

From the ideal gas law:

$$P_o = \rho_o R T_o$$

we get:

$$\Delta P_i = 2\sqrt{\pi}\, R\rho_o \sqrt{T_i T_o}\, s \; .$$

Which, for ambient density, is:

$$\rho_o = \frac{\Delta P_i}{2\sqrt{\pi}\, R \sqrt{T_i T_o}\, \dfrac{V \cos \alpha}{u_o}} \qquad (3.1.4)$$

substituting $u = \sqrt{2kT/m}$, and rearranging yields:

$$\rho_o = \frac{\Delta P_i}{\sqrt{\pi}\, u_i\, V \cos \alpha} \quad \text{(see Ref. 4)} \; . \qquad (3.1.5)$$

Figure 6 gives typical values for $P_{i_{max}}$, $P_{i_{min}}$, and P_o for a typical Aerobee 300 trajectory.

3.2 AMBIENT TEMPERATURE VS. ALTITUDE—SCALE HEIGHT METHOD

The determination of ambient gas temperature from pressure measurements in a moving and tumbling pressure gauge can be accomplished by two independent methods. One method is the determination of a scale height for the ambient gas; the other uses the "velocity scan" technique,[3] which determines the relationship between the vehicle velocity, a known parameter, and the most probable thermal velocity of the ambient particles, a quantity proportional to the square root of the temperature.

For the first method, we assume an atmosphere at equilibrium such that the hydrostatic equation holds:

$$\frac{dP}{dh} = -\rho g \quad . \tag{3.2.1}$$

Also, we assume the ideal gas law is valid:

$$P = \rho RT \quad . \tag{3.2.2}$$

Differentiating Eq. (3.2.2) with respect to altitude, we get:

$$\frac{dP}{dh} = RT \frac{d\rho}{dh} + \rho R \frac{dT}{dh} \quad . \tag{3.2.3}$$

Substituting Eq. (3.2.3) into Eq. (3.2.1):

$$RT \frac{d\rho}{dh} + \rho g + \rho R \frac{dT}{dh} = 0$$

or

$$RT \frac{d\rho}{dh} + \rho \left(g + R \frac{dT}{dh} \right) = 0 \quad . \tag{3.2.4}$$

For the TP experiment, the expression for ambient density was derived previously:

$$\rho = \frac{\Delta P_i}{U_i \sqrt{\pi}\ V \cos \alpha} \quad . \tag{3.2.5}$$

Now

$$\frac{d\rho}{dh} = \frac{1}{U_i \sqrt{\pi}\ V \cos \alpha} \left[\frac{d\Delta P_i}{dh} - \frac{\Delta P_i}{V} \frac{dV}{dh} + \tan \alpha\ \Delta P_i \frac{d\alpha}{dh} \right] \quad . \tag{3.2.6}$$

Substituting Eqs. (3.2.5) and (3.2.6) into Eq. (3.2.4) and concelling common terms

$$T = -\left(\frac{g}{R} + \frac{dT}{dh} \right) \frac{\Delta P_i}{\frac{d\Delta P_i}{dh} - \frac{\Delta P_i}{V} \frac{dV}{dh} + \tan \alpha\ \Delta P_i \frac{d\alpha}{dh}} \quad . \tag{3.2.7}$$

This expression relates the ambient temperature to the basic pressure measurement and trajectory information. To change the equation to a form

more suitable for data reduction, we multiply the numerator and denominator by $V_Z = dh/dt$,

$$T = -\left(\frac{g}{R} + \frac{dT}{dh}\right) \frac{\Delta P_i \, V_Z}{\frac{d\Delta P_i}{dt} - \frac{\Delta P_i}{V}\frac{dV}{dt} + \tan\alpha \, \Delta P_i \frac{d\alpha}{dt}} \quad . \quad (3.2.8)$$

Equation (3.2.8) allows one to reduce much of the data, in terms of flight time, from the original telemetry records, eliminating trajectory information requirements until final analysis.

Returning to Eqs. (3.2.1) and (3.2.2), we see that Eq. (3.2.1) can be expressed as:

$$P_1 - P_2 = \int_{h_2}^{h_1} \rho g dh \quad . \quad (3.2.9)$$

Where P_1 is the ambient pressure at altitude h_1 and P_2 is the ambient pressure at altitude h_2.

From Eq. (3.2.2), we can express ambient temperature as:

$$T = P/\rho R \quad .$$

Therefore,

$$T_1 = \frac{\int_{h_2}^{h_1} \rho g dh + P_2}{\rho_1 R} \quad . \quad (3.2.10)$$

P_2 can be determined by

$$T_2 = P_2/\rho_2 R \quad .$$

Where T_2 is obtained from the data using Eq. (3.2.8).

Equations (3.2.8) and (3.2.10) are both valid for the assumption of Eqs. (3.2.1) and (3.2.2). Both equations have been used for data reduction and excellent agreement in the results is obtained.

Another technique for temperature determination which is independent of Eq. (3.2.1) is discussed in the following section.

3.3 AMBIENT TEMPERATURE VS. ALTITUDE—VELOCITY SCAN METHOD

The velocity scan method for determining ambient temperature has been derived previously and is reported in Ref. 3. For this the thermal transpiration equation is used.

$$\frac{P_i}{P_o} = \sqrt{T_i/T_o}\ f(s) \qquad (3.3.1)$$

Since the TP is tumbling in a plane whose angle from the velocity vector is α, the angle of attack, β, for any given pressure reading is:

$$\cos\beta = \cos\alpha \cos\theta$$

where θ is the rotation angle in degrees in the plane of tumble. θ is zero when $\beta = \alpha$, and a peak pressure reading is obtained. For any given tumble period, it can be assumed that the ambient temperature is constant, therefore, the ratio of (3.3.1) at β_1, to (3.3.1) at β_2 yields:

$$(P_{i_{\beta_1}}/P_{i_{\beta_2}}) = f(s_{\beta_1})/f(s_{\beta_2}) \qquad (3.3.2)$$

where

$$f(s) = e^{-s^2} + \sqrt{\pi}\, s(1+\mathrm{erf}s)$$

$$s_1 = V \cos\alpha \cos\theta_1/u_o$$

$$u_o = \sqrt{2kT_o/m}$$

As is known:[3]

$$\lim_{s\to\infty} f(s) = 2\sqrt{\pi}\, s.$$

Therefore, for high S ($s > 2$), the linearity of f(s) causes:

$$P_{i_{\beta_1}}/P_{i_{\beta_2}} = \cos\theta_1/\cos\theta_2.$$

However, if the 90° point ($\theta = 90°$), for example, and the peak pressure point ($\theta = 0°$) are chosen for the pressure reading.

$$P_{i_\alpha}/P_{i_{90^\circ}} = f(S_\alpha) \quad . \qquad (3.3.3)$$

From this ratio, an S can be determined. The ambient temperature is then given by:

$$T_o = \frac{m}{2k}\left(\frac{V \cos \alpha}{s_\alpha}\right)^2 \qquad (3.3.4)$$

where V, s, α, m and k are known quantities.

It will briefly be noted here that the errors involved in reducing data from Eq. (3.3.4) above become quite large for high vehicle velocities, since all the temperature information is contained at points on the pressure curve near $\theta = 90^\circ$, where S is small (Fig. 7). Also, the inherent inaccuracy of a linear amplifier at low outputs, compared to full scale outputs, causes errors in P_{90° that appear to approach and even exceed 100% especially when background pressure effects are also present. A thorough error analysis of this technique has been initiated and will be reported separately when completed. Therefore, the data presented in a later section was reduced using the previous method (scale height). In either case, assuming the gauge has a linear pressure-current characteristic, a systematic calibration error does not cause an error in the computed ambient temperature, since only ratios of the measured pressures are involved in the expressions used.

4. DATA PRESENTATION

The following data were obtained from NASA 6.06, launched at Wallops Island, Virginia, on November 20, 1962 at 21:41:30 GMT. The launch vehicle, an Aerobee 300, obtained a peak altitude of 344 km.

The pressure sensor used in this experiment was an omegatron partial pressure gauge,[5] tuned to measure N_2 partial pressure.

This first experiment was, at least partially, intended for the purpose of system evaluation. As indicated by the data, the TP operated as expected and all instrumentation functioned properly. The major limitation on data aquisition was caused by the outgassing of the omegatron gauge. Figure 8 shows a plot of background pressure vs. flight time. It is interesting to note here that the minimum pressure attained during the preflight pump down of the gauge was approximately 10^{-6} mm Hg. As can be seen in Fig. 8, only a factor of 5 in the reduction of this pressure was obtained during the flight, even though the effective pumping speed was considerably increased. Consequently, meaningful data were obtained to only 260 km where the background pressure became large compared to the ambient pressure.

Figure 9 is a picture of a portion of the telemetry record from NASA 6.06. Figures 10 and 11 are the resulting ambient density and temperature, respectively. These data were obtained by measuring the peak pressure points ($P_{i_{max}}$) and the background pressure (P_{BG}), smoothing both data curves independently, and then subtracting the smoothed background pressure from the smoothed peak pressure to obtain the ΔP_i. In general, the spread in data for both the peak pressure values and background pressure values is a maximum of ±2.5% from the smoothed curves. Therefore, the possible uncertainty in ΔP_i; i.e., $P_{i_{max}}-P_{BG}$, increases with altitude as $P_{i_{max}}$ approaches P_{BG}. A curve of possible uncertainty vs. altitude for NASA 6.06 data is given in Fig. 12 for a ±2.5% spread in $P_{i_{max}}$ and P_{BG}. As can be seen, the maximum possible uncertainty in ΔP_i is approximately 28% (±14% from the mean value) at 235 km for the upleg data. At 220 km the possible uncertainty is 16% (±8% from the mean value). In general, data are considered useless when the possible uncertainty is above 30%. Since the convergence to ±5% data occurs within about 40 km from the point where data reduction is discontinued, the extension of the density data through the region of maximum uncertainty with the assumption that the atmosphere is approximated isothermal, yields density which can be considered better than ±14% at the point where data reduction is discontinued.

The difference between upleg and downleg density for NASA 6.06 is unexplained as yet. As discussed in the previous paragraph, the difference

is not attributed to uncertainty in data since: (1) both profiles produce almost the same temperature in the high altitude part of the data (equal scale height); (2) all engineering parameters for the instrumentation were the same for upleg and downleg data; and (3) confidence in the angle of attack data is set at about ±5°. An error of approximately 45° would be required to produce the difference seen.

Since NASA 6.06 was fired toward the east at local sunset, a geophysical explanation of the difference in upleg and downleg density is inviting. However, until more data are obtained and the problem is viewed in perspective with profiles obtained at other times during the day and night, a geophysical explanation would be pure conjecture.

Density and temperature profiles for NASA 6.07 and NASA 6.08 are given in Figs. 13 through 16. As can be seen, data were obtained to higher altitudes for both 6.07 and 6.08 than was obtained for 6.06, due to a lower background pressure in the last two experiments. The trajectories for the last two experiments were similar to 6.06, with a peak altitude of approximately 340 km.

NASA 6.07 was fired during a pass of Explorer XVII to measure atmospheric parameters at the same time and position in space as the aeronomy satellite. The firing was a complete success, with the satellite orbit passing under the sounding rocket trajectory. Preliminary comparison of the rocket data with the satellite data has shown good agreement.

NASA 6.08 was fired during the July 20, 1963, eclipse. An attempt was made to measure a helium density profile on the upleg portion of the trajectory. The results were that the atmospheric helium density was less than the detection capability of the instrumentation, i.e., less than 1 part in 100 of total density. The N_2 density profile was produced from the downleg data.

REFERENCES

1. Carignan, G. R. and Brace, L. H., The Dumbbell Electrostatic Ionosphere Probe: Engineering Aspects, Univ. of Mich., ORA Report 03599-6-S, Ann Arbor, November 1961.

2. Albus, J. S., A Digital Solar Aspect Sensor, NASA Technical Note D-1062, September 1961.

3. Schultz, F. V., Spencer, N. W., and Reifman, A., Atmospheric Pressure and Temperature Measurement Between the Altitude of 40 and 110 Kilometers, Upper-Air Research Program, Report No. 2, Univ. of Mich. Res. Inst. Report, Ann Arbor, July 1948.

4. Horowitz, R. and LaGow, H. E., Upper Air Pressure and Density Measurements from 90 to 220 Kilometers With the Viking 7 Rocket, Journal of Geophysics Research, 62:57-78 (1957).

5. Nagy, A. F., et al., Measurements of Atmospheric Pressure, Temperature, and Density at Very High Altitudes, Univ. of Mich., ORA Report 02804-7-F, August 1961.

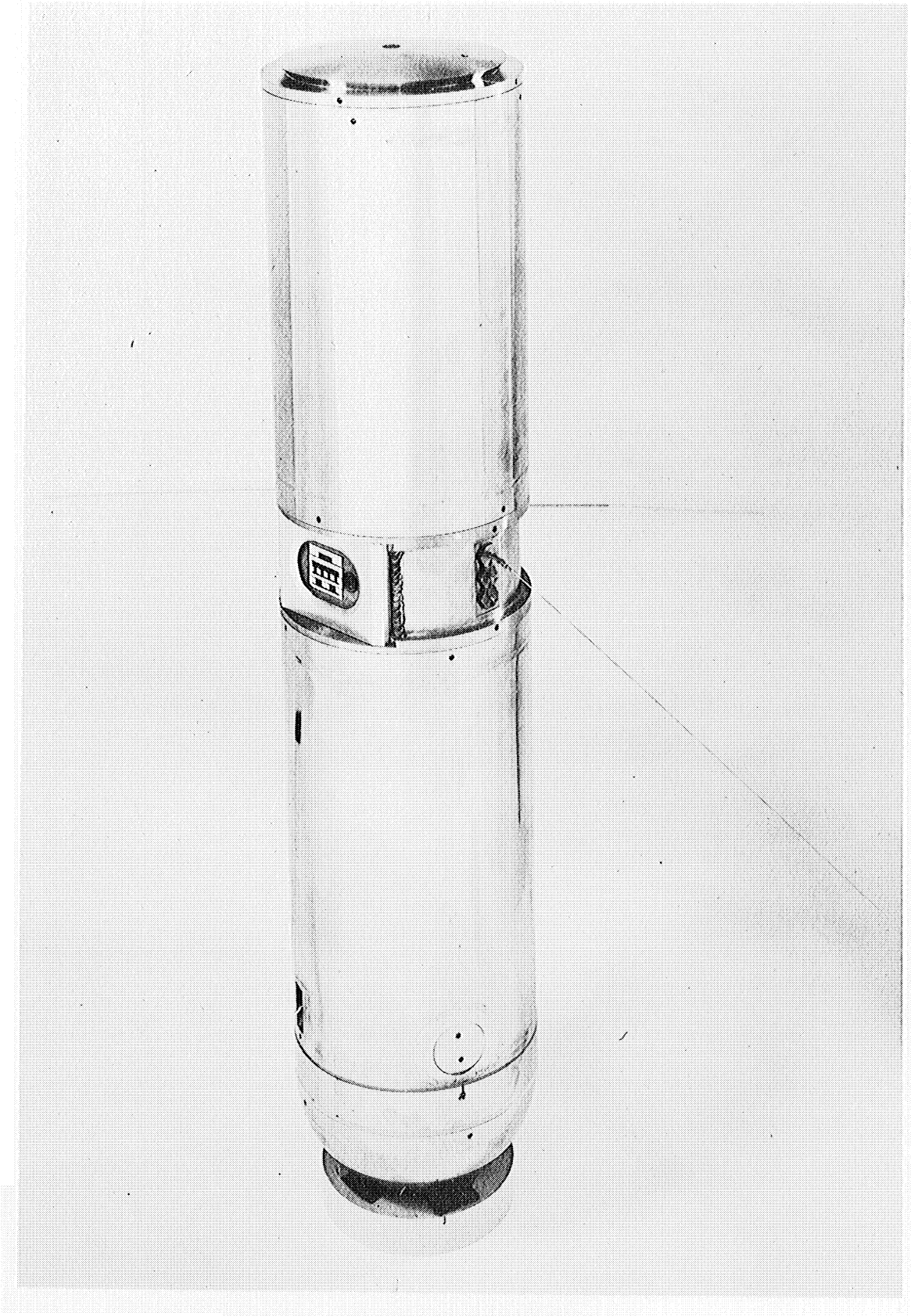

Fig. 1. The thermosphere probe.

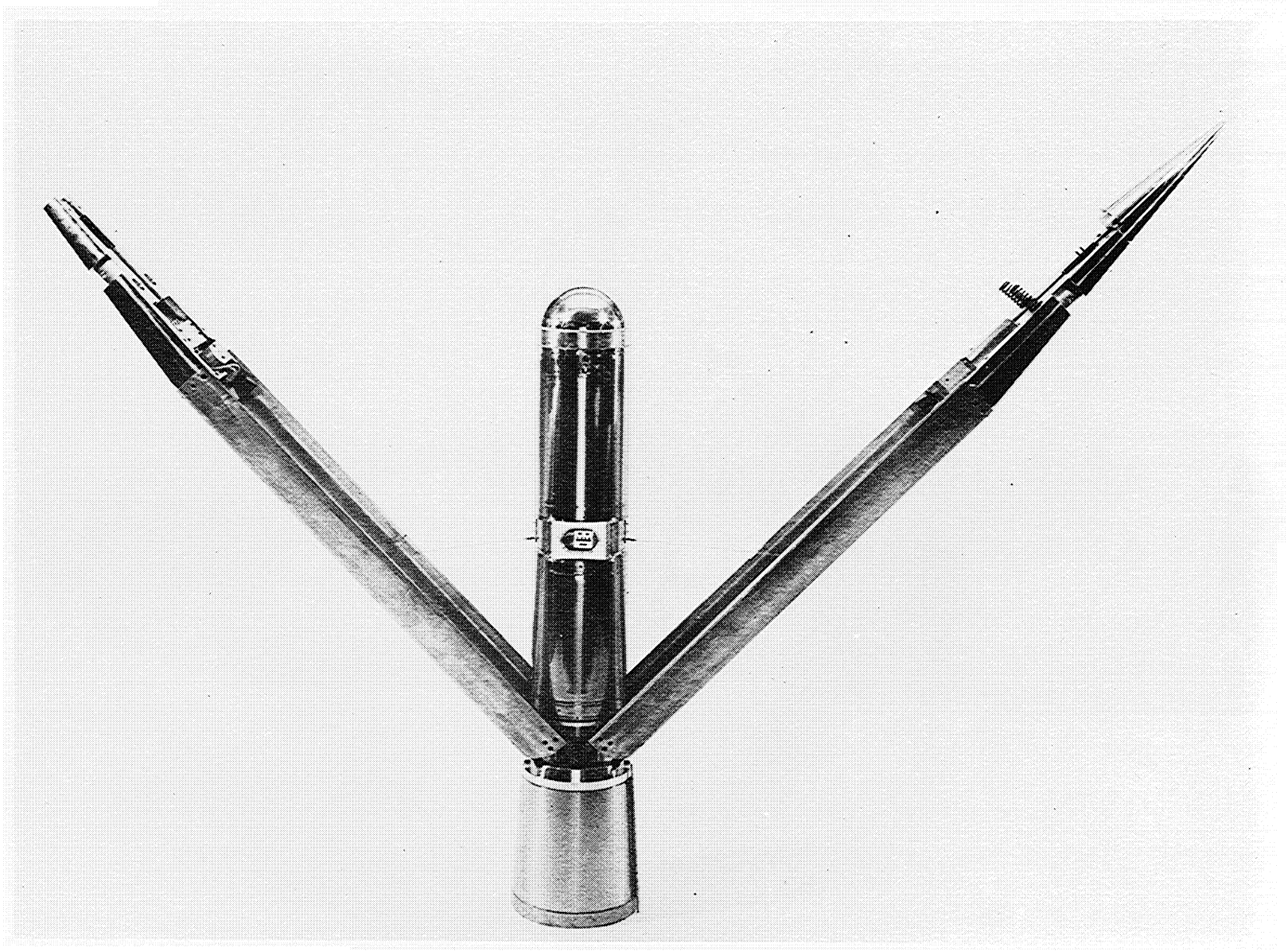

Fig. 2. Probe in ejection nose cone.

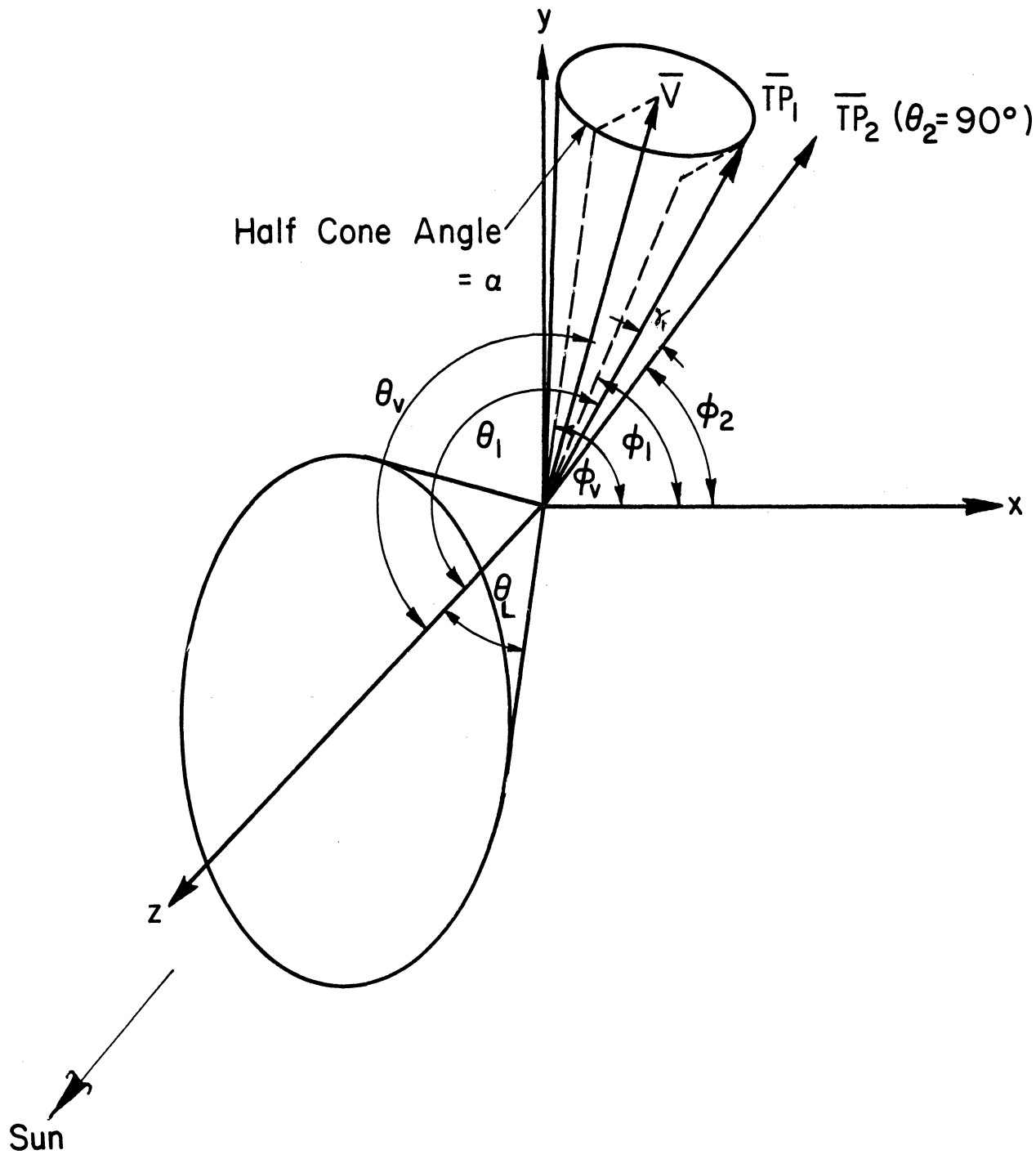

Fig. 3. Inertial frame coordinate system.

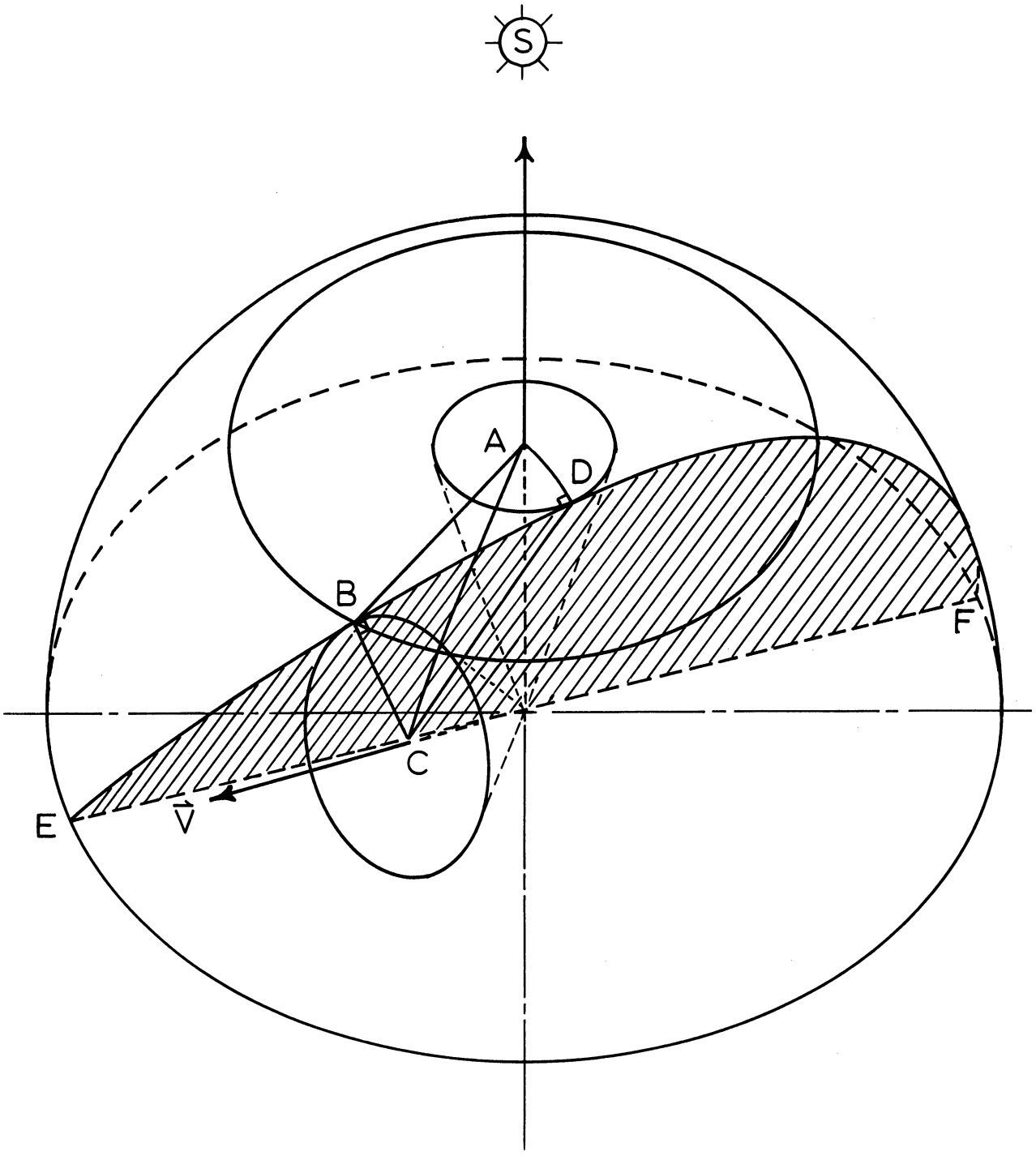

Fig. 4. Hemispherical analysis geometry.

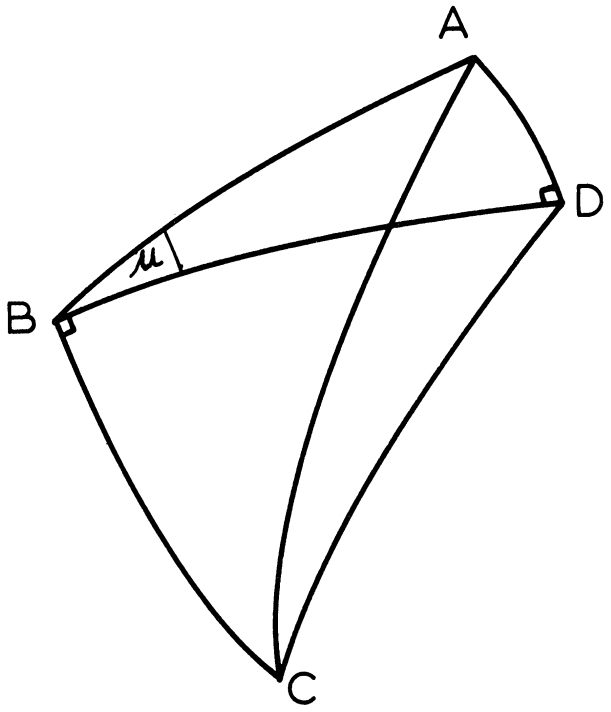

Fig. 5. Spherical triangles.

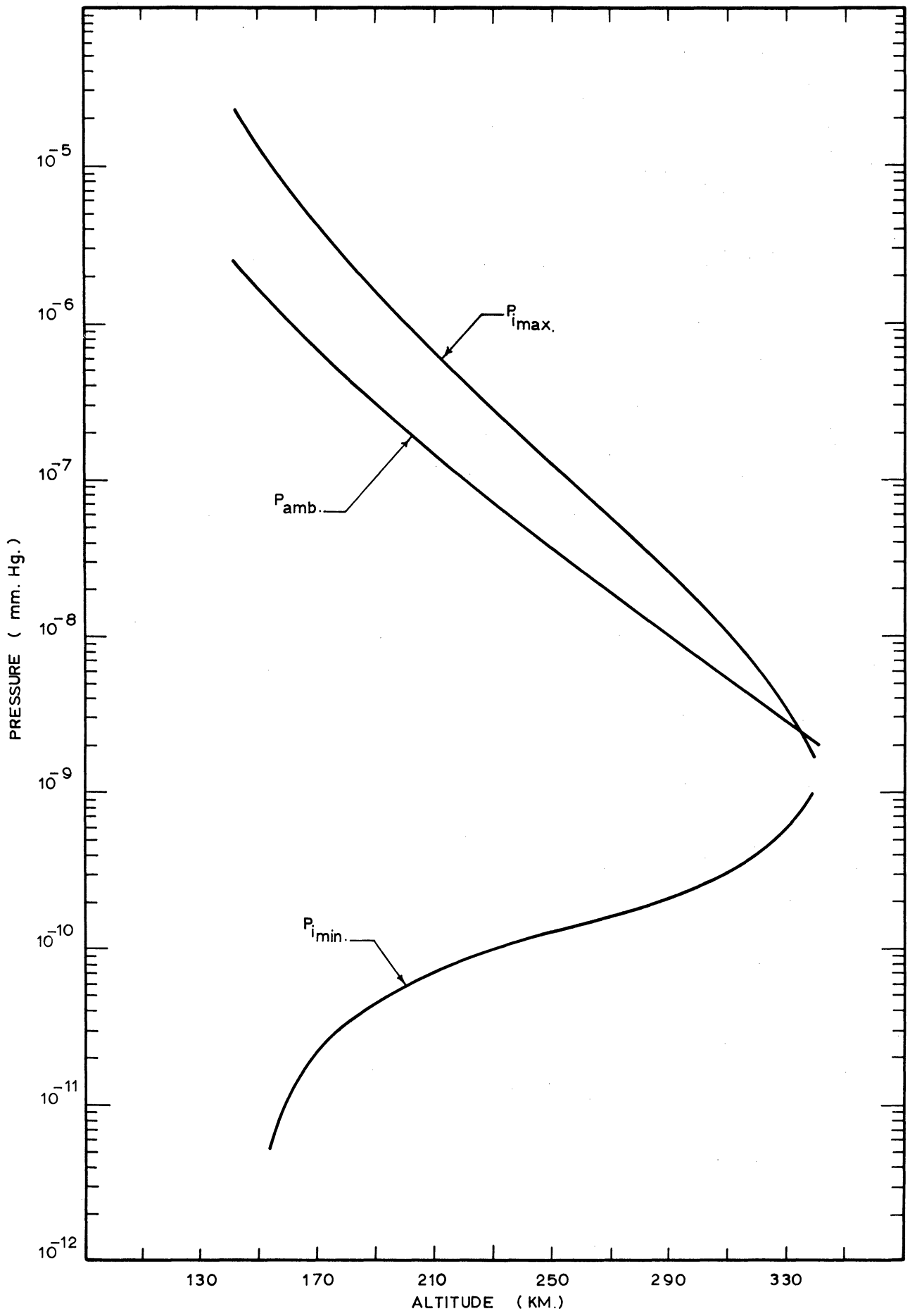

Fig. 6. Pressure relationships for Aerobee 300 trajectory.

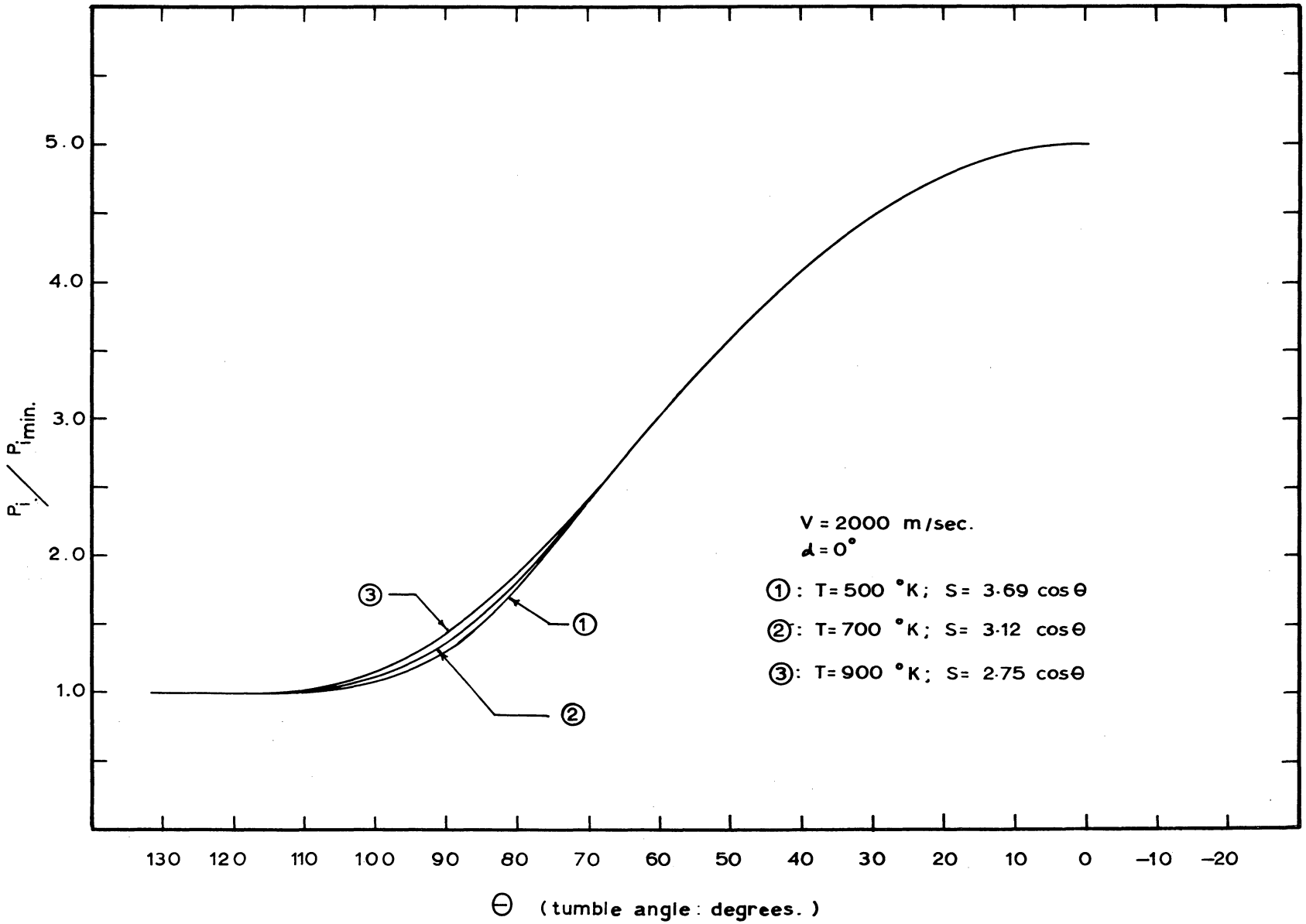

Fig. 7. Temperature effect on P_i vs. θ.

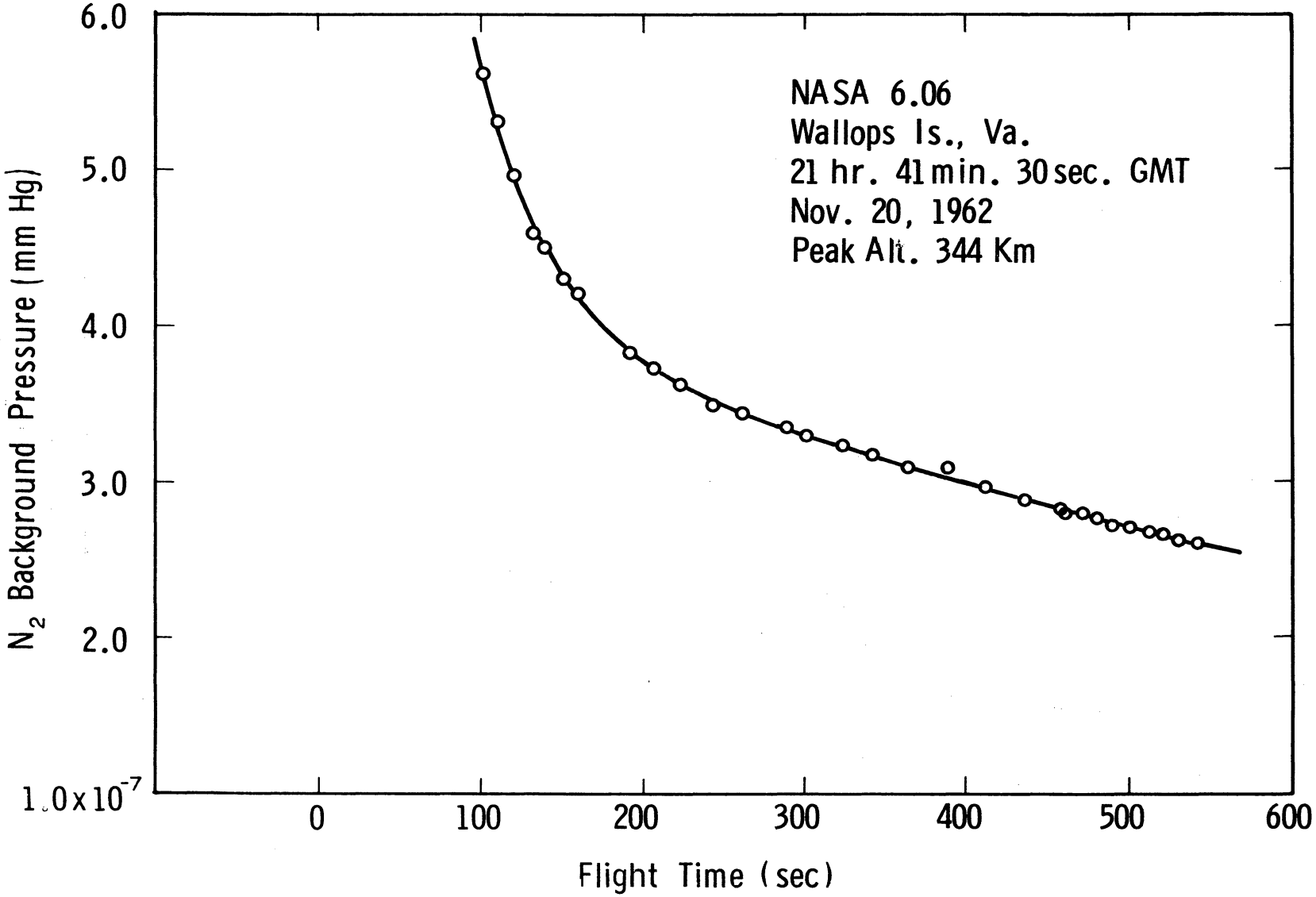

Fig. 8. Background pressure vs. flight time—NASA 6.06.

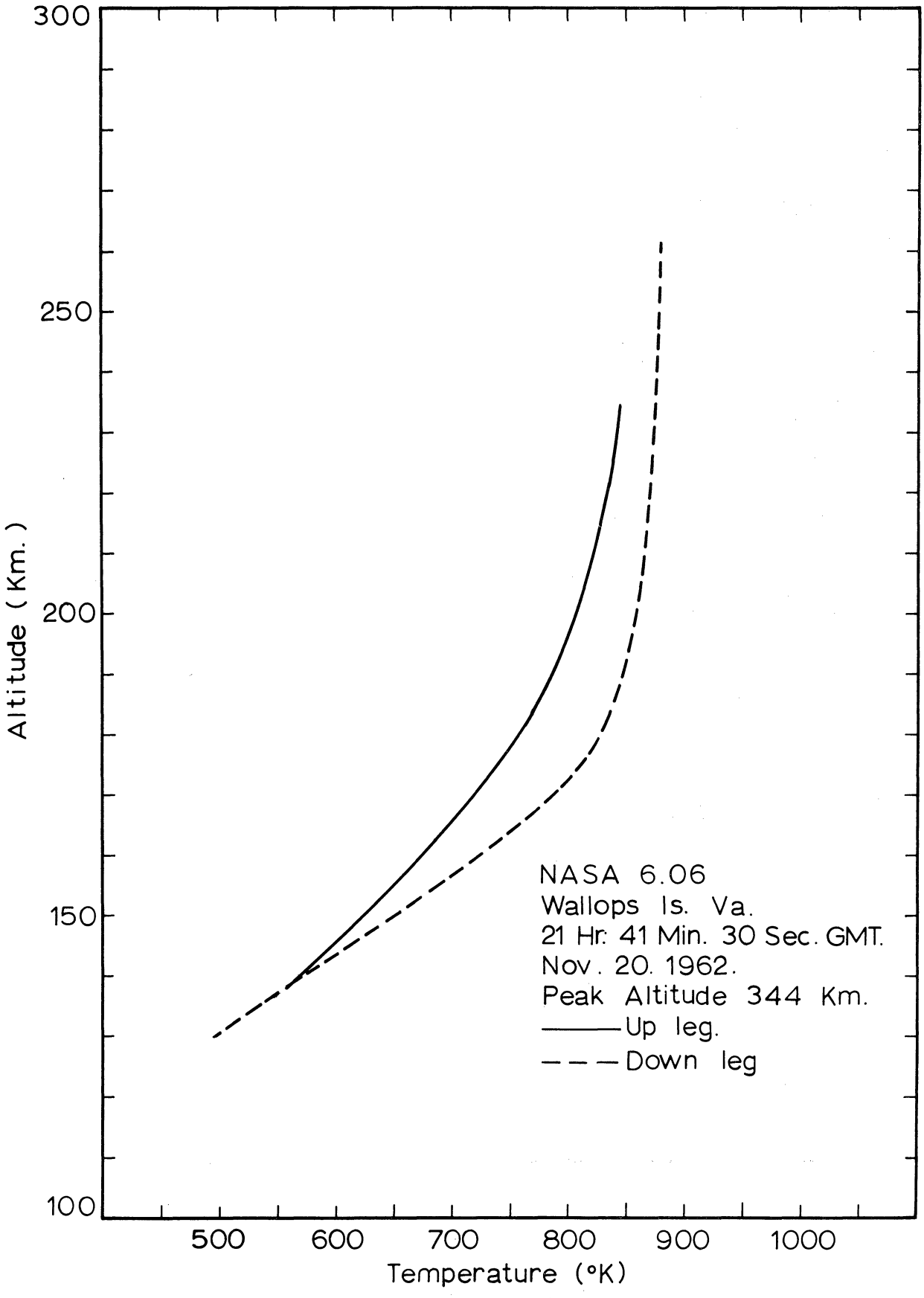

Fig. 11. Ambient temperature vs. altitude—NASA 6.06.

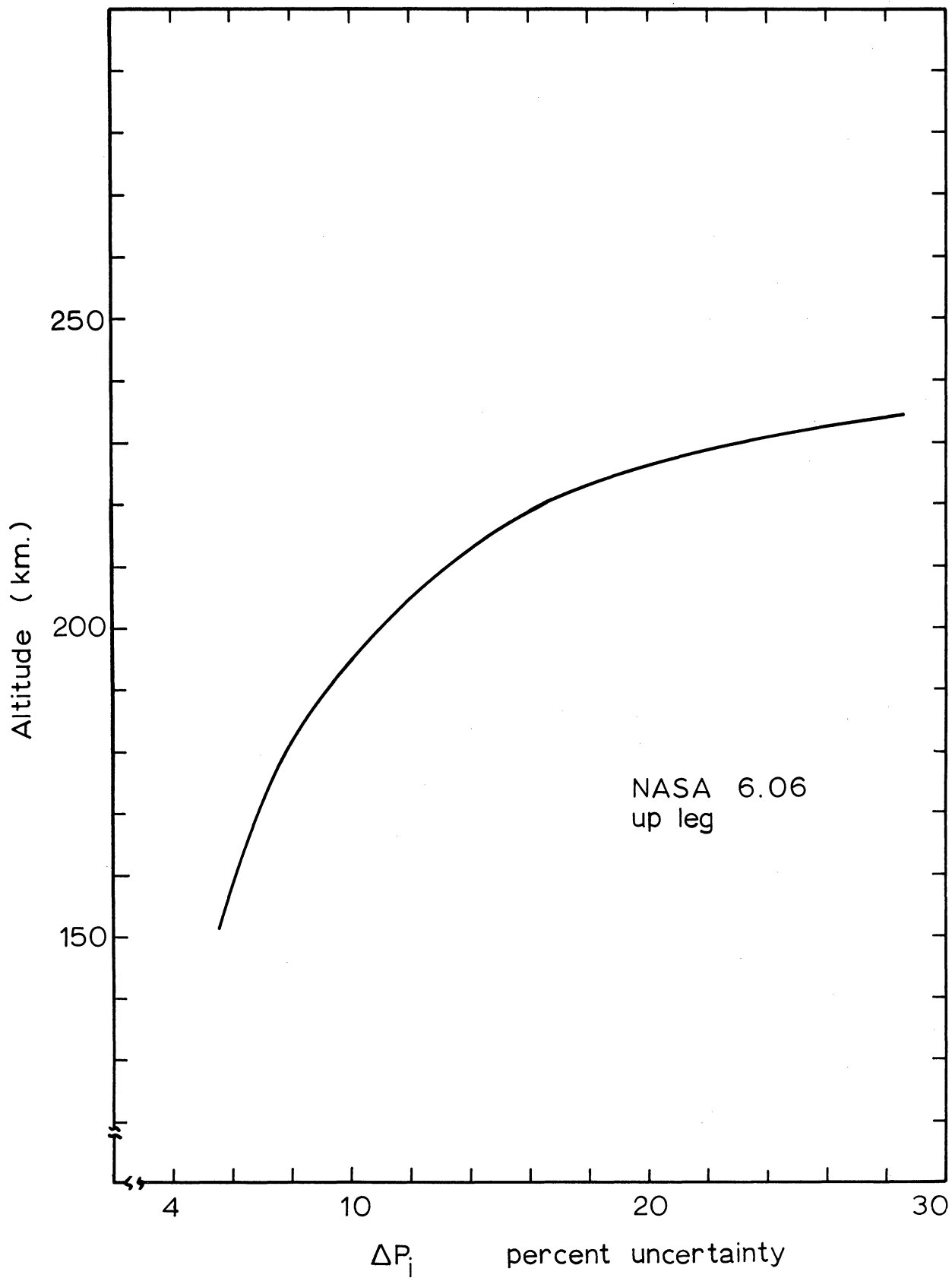

Fig. 12. Possible uncertainty in ΔP_i vs. altitude—NASA 6.06.

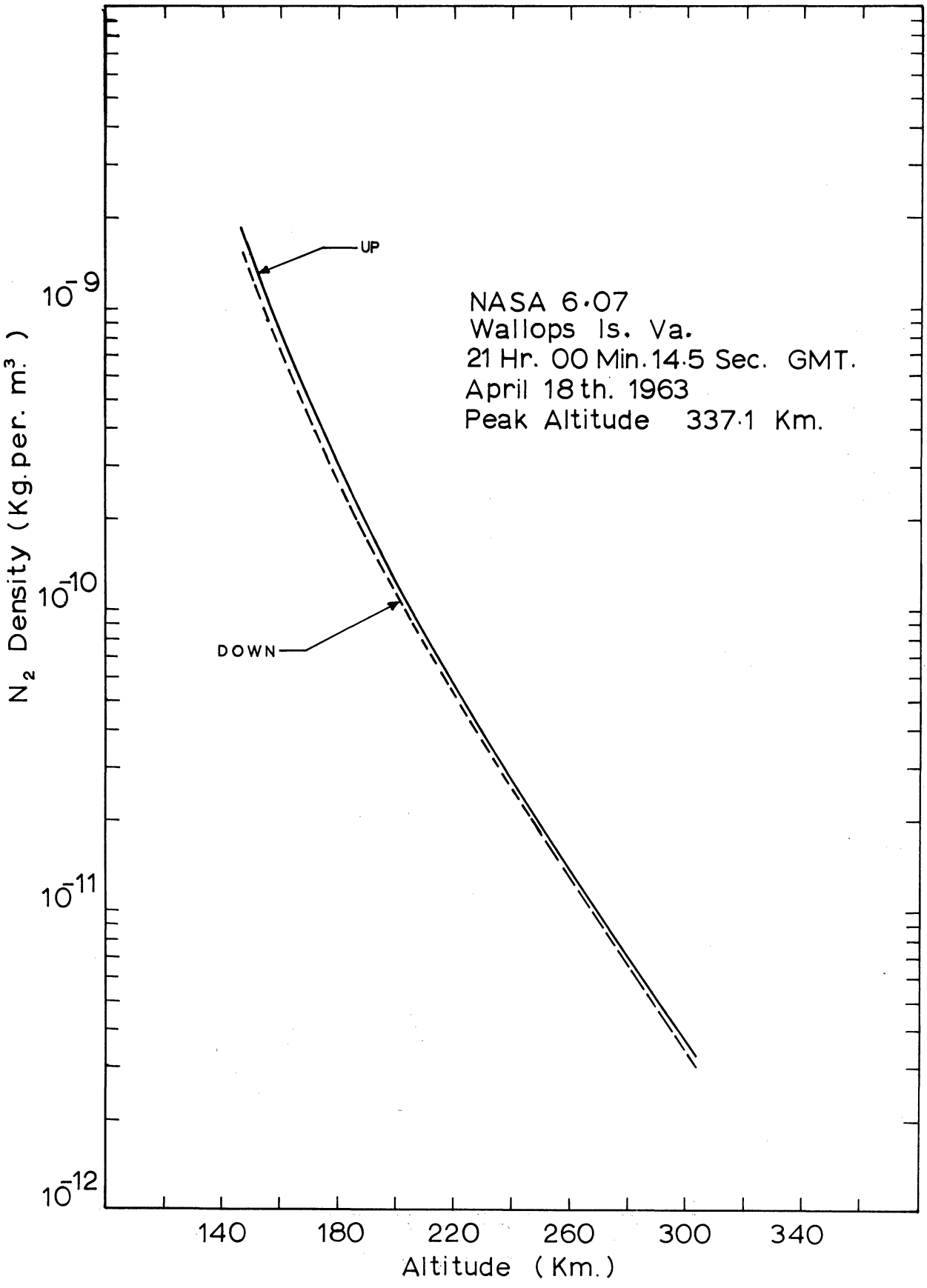

Fig. 13. Density vs. altitude—NASA 6.07.

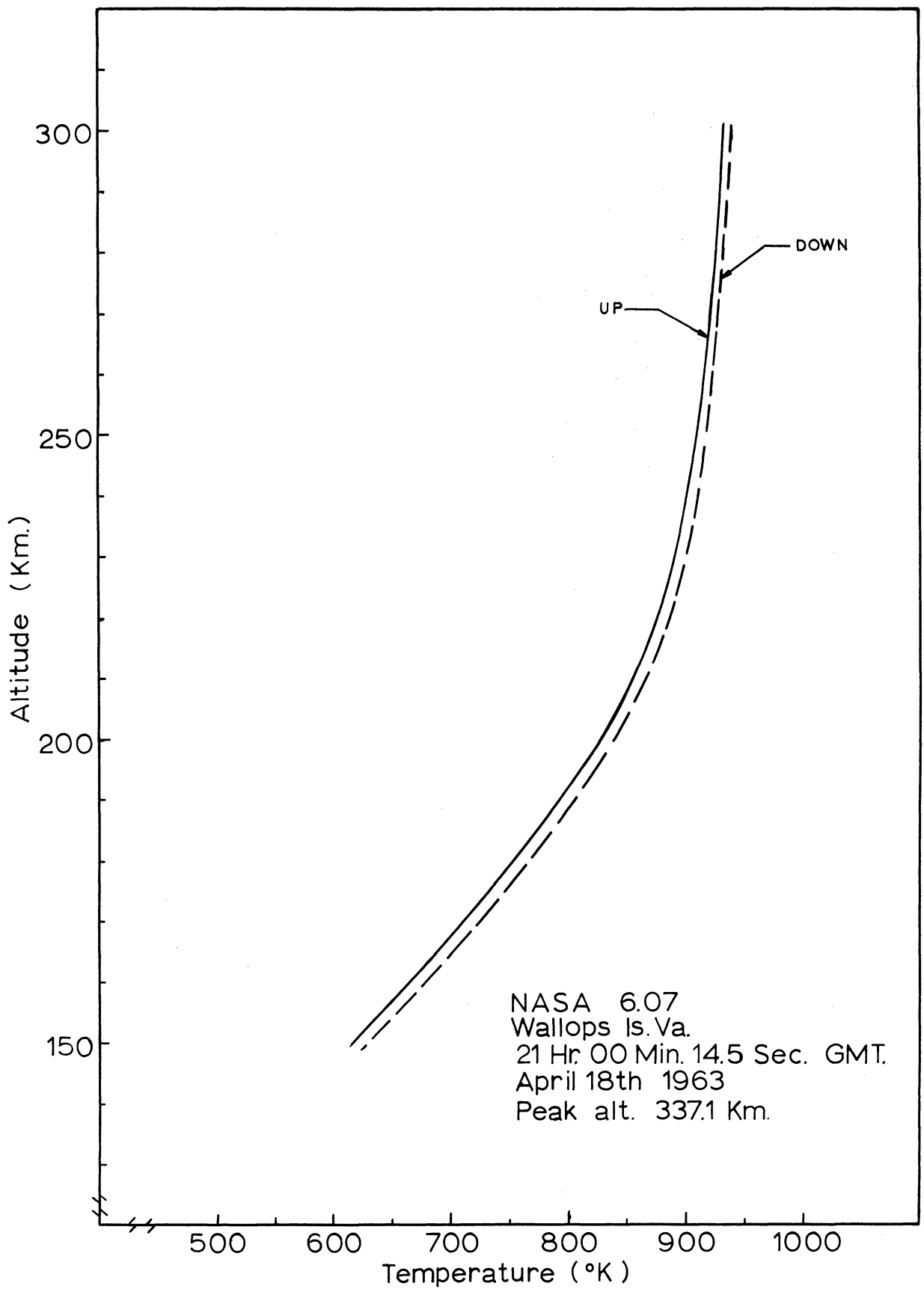

Fig. 14. Temperature vs. altitude--NASA 6.07.

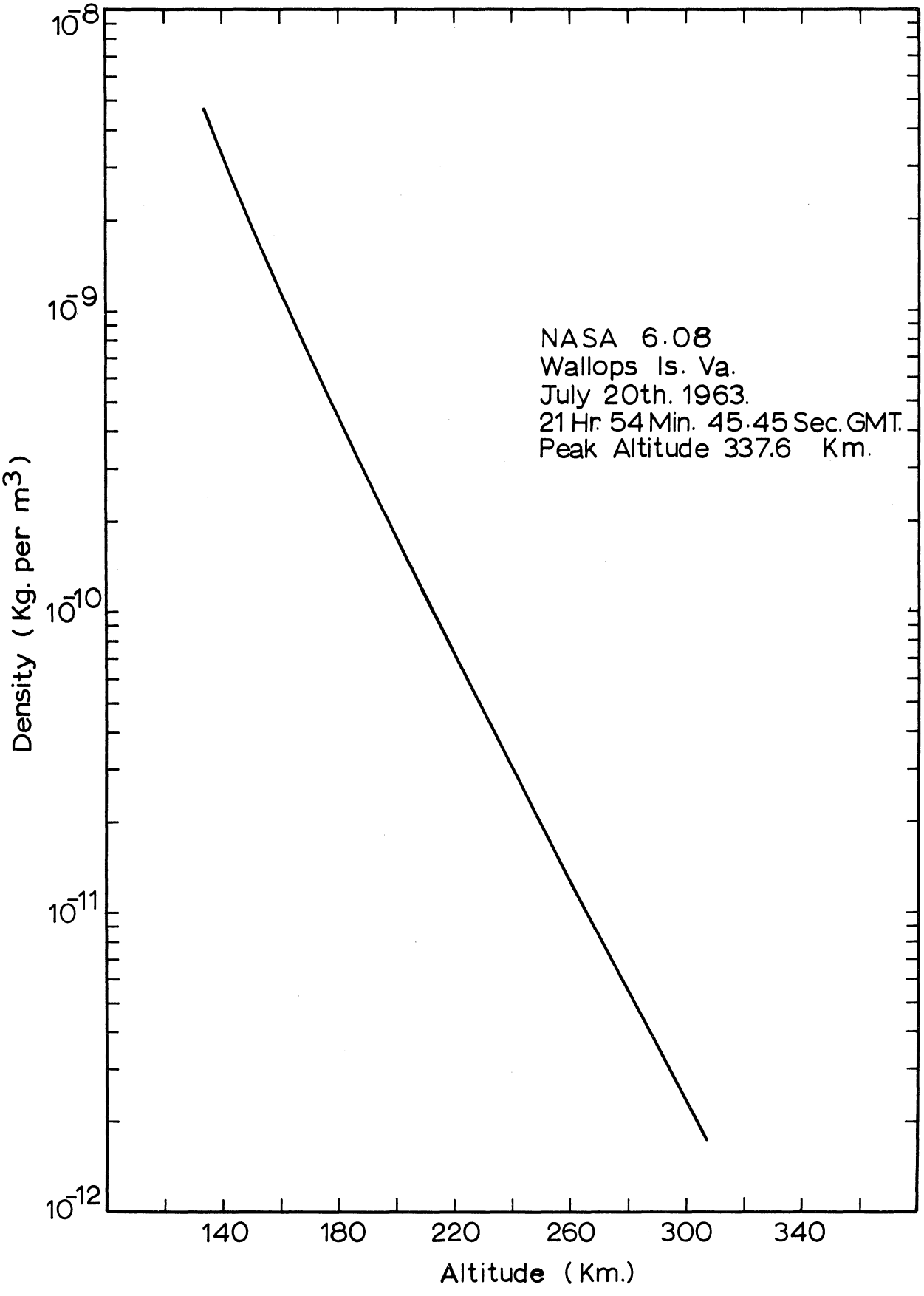

Fig. 15. Density vs. altitude—NASA 6.08.

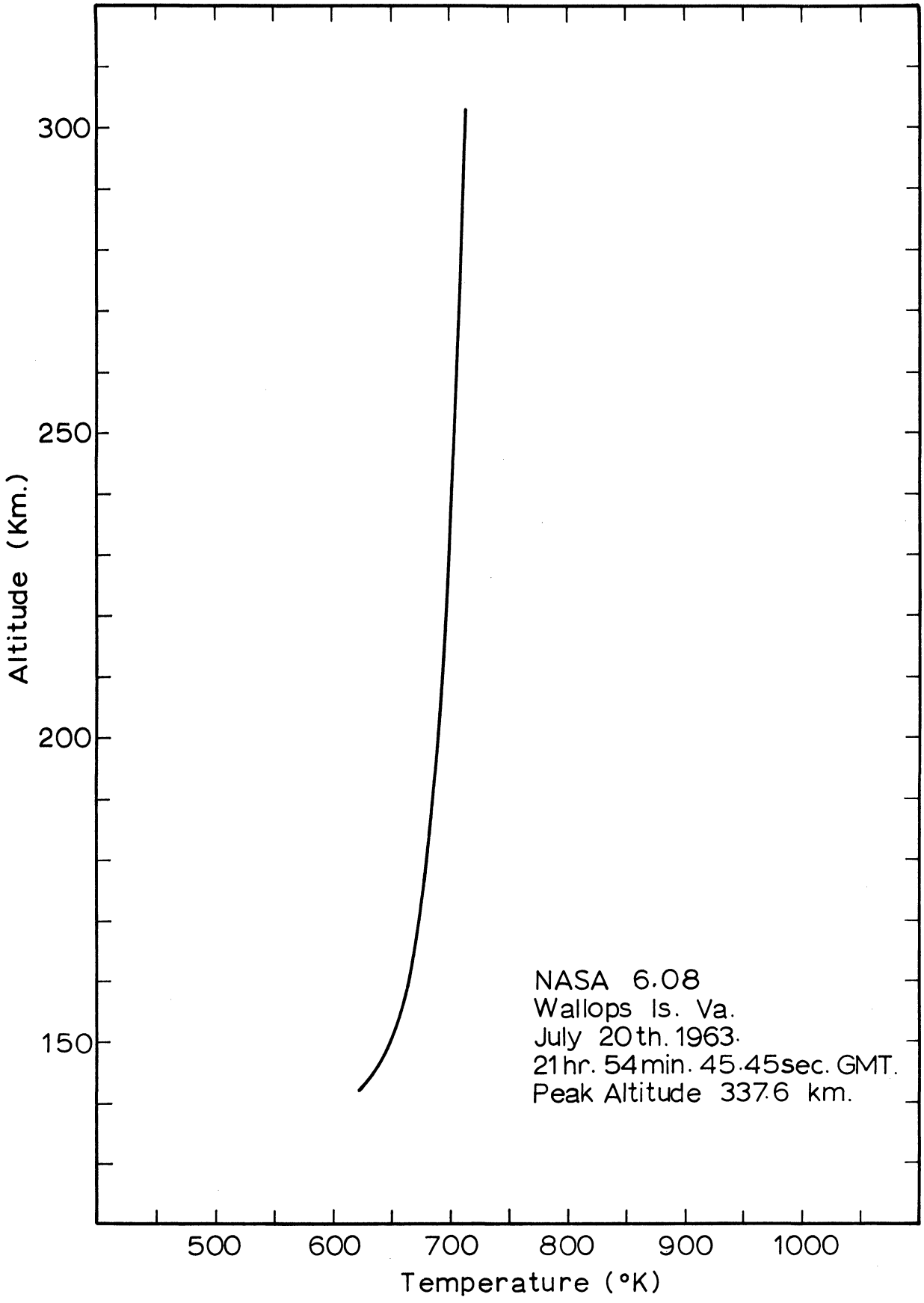

Fig. 16. Temperature vs. altitude—NASA 6.08.

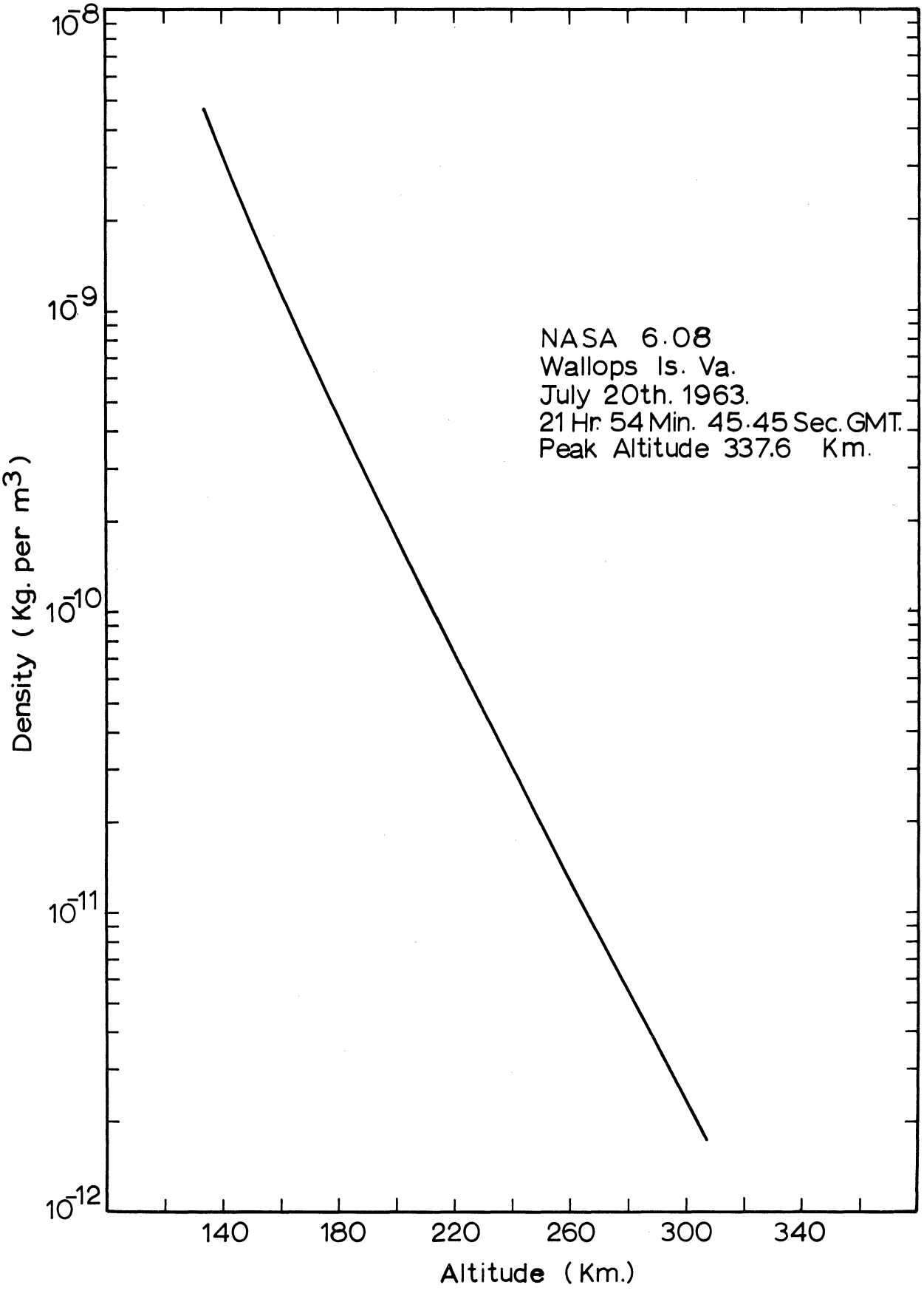

Fig. 15. Density vs. altitude—NASA 6.08.

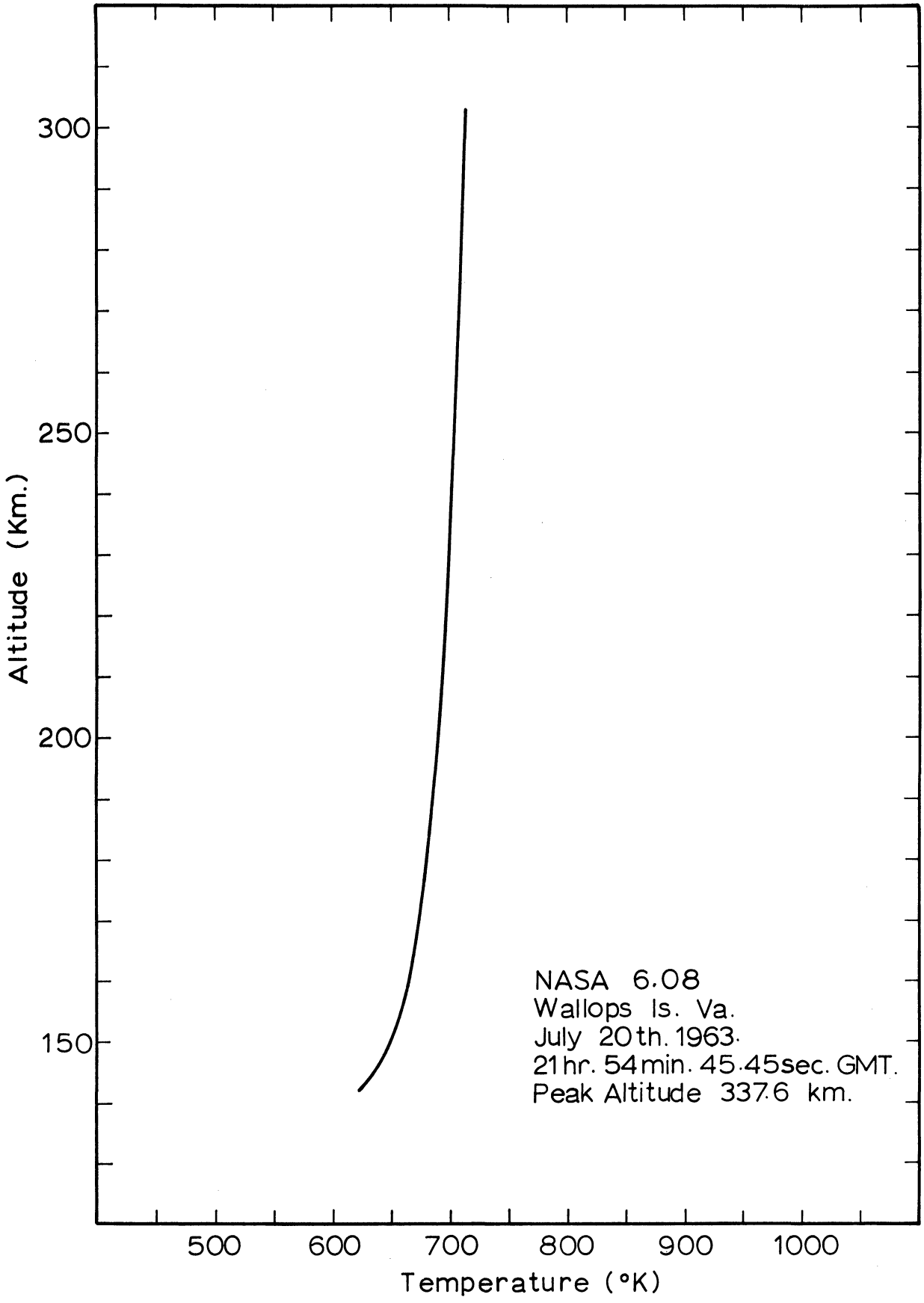

Fig. 16. Temperature vs. altitude—NASA 6.08.